

A method to remotely measure temperature change in a lithium niobate crystal using birefringence

Daniel Sando
d.sando@qut.edu.au

Applied Optics Program, Queensland University of Technology, GPO Box 2434,
Brisbane QLD 4001, Australia

Esa Jaatinen

Applied Optics Program, Queensland University of Technology, GPO Box 2434,
Brisbane QLD 4001, Australia

We present a non-contact method of determining temperature change in a lithium niobate crystal. The technique has the advantage of being simple to implement and offers a precision at least as good as conventional temperature measurement methods over large ranges (~ 200 K). A novel application of this technique involves measuring temperature in different regions of the crystal simultaneously, which could be useful for determining stresses and heat diffusion parameters. The technique could be successfully applied to monitor crystal temperature for thermal fixing of holograms or related applications. [DOI: 10.2971/jeos.2009.09011]

Keywords: birefringence, lithium niobate, temperature sensing, thermal fixing

1 INTRODUCTION

The photorefractive crystal Lithium Niobate (LiNbO_3) is extensively used in three dimensional optical data storage research; particularly in the area of holographic data storage [1]. This technique of storing data involves recording data as phase holograms by the photorefractive effect. Data can also be stored by using an amplitude mask to record data as bits [2]. Here each bit of data is stored as a change in the refractive index in a particular region of the crystal that can subsequently be read out.

One of the disadvantages of photorefractive media as data storage materials is that during readout, the stored data may be erased by the readout beam. One technique for overcoming this in LiNbO_3 is to thermally fix the data. This process is based on replacing the space charge field grating with an ionic grating which is resilient to the readout beam.

Thermal fixing requires that the crystal be heated to temperatures > 400 K (either during or after recording) so that ions are made mobile [3, 4]. Generally these are hydrogen ions (protons) [5] with a thermal activation energy of ~ 1.1 eV [6]. Once mobile, these ions migrate to neutralise the induced space charge field. Upon readout, the space charge field is erased, but the ionic grating remains because it is not affected by light. The temperature at which thermal fixing occurs is known to significantly impact factors such as the diffraction efficiency of holograms [7]. Therefore, it must be accurately known to optimise the data storage process in photorefractive lithium niobate.

Direct measurement of the temperature of the medium with contact probes can be problematic due to the temperatures involved and conductivity issues between probe and medium.

To overcome these problems, some form of non-contact temperature measurement is therefore desirable.

In this paper we present a non-contact optical method for determining temperature change in a LiNbO_3 crystal, using a single HeNe laser and photodetector. Here we use the temperature dependence of the birefringent optical properties of LiNbO_3 [8] to determine the medium temperature. The present work verifies the effectiveness of the technique by providing experimental evidence and a theoretical determination of the accuracy is possible. In a novel application of this technique, we show how it can be applied to measure the temperature gradients inside the crystal. In this case, a CCD camera is used to simultaneously measure temperature in different areas of the crystal. The methodology described can be applied to other birefringent crystals that have temperature dependent optical properties.

2 THEORY

Birefringence is a property of crystals with a uniaxial structure that results in different refractive indices for a light field polarised in a direction perpendicular to, and parallel with, the optic axis [9]. In lithium niobate the magnitude of the birefringence is ~ 0.08 for visible wavelengths and this value is dependent on temperature [10].

When the input beam is linearly polarised at an angle ϕ to the crystal's optic axis, upon entering the crystal, the field can be split into ordinary and extraordinary components as

$$E_{in} = E_0 \sin \phi \hat{\mathbf{o}} + E_0 \cos \phi \hat{\mathbf{e}} \quad (1)$$

where E_0 is the initial field amplitude, $\hat{\mathbf{o}}$ is a unit vector normal to the crystal's optic axis, and $\hat{\mathbf{e}}$ is a unit vector in the

direction of the optic axis. As the field propagates through the crystal of thickness d the ordinary and extraordinary components traverse different optical paths dependent on the value of n_o and n_e respectively. Thus the field at the output face can be expressed as

$$E_{out} = E_0 e^{-\frac{\gamma d}{2}} \left(\sin \phi e^{-jkdn_o} \hat{\mathbf{o}} + \cos \phi e^{-jkdn_e} \hat{\mathbf{e}} \right) \quad (2)$$

where γ is a constant that incorporates attenuation effects, such as absorption, scattering, beam fanning etc., $k = 2\pi/\lambda$ is the wave number, and n_o and n_e are the ordinary and extraordinary refractive indices respectively. If a polariser, with its axis of polarisation at an angle θ to the crystal's optic axis, is placed between the exit face of the crystal and a photodetector, the intensity at the photodetector is given by

$$I_{det} = I_0 e^{-\gamma d} \left\{ \left(\sin \phi \sin \theta + \cos \phi \cos \theta \right) + \left(2 \sin^2 \phi \sin^2 \theta \cos^2 \phi \cos^2 \theta \cos [kd\Delta n] \right) \right\} \quad (3)$$

Here, $I_0 = E_0^2$ is the initial intensity of the beam before passing through the crystal, and $\Delta n = n_o - n_e$ is the birefringence. A change in temperature changes the values of d and Δn . Thermal expansion of the material modifies d according to [11]

$$d = d_{298} \left(1 + \alpha (T - 298) + \beta (T - 298)^2 \right) \quad (4)$$

where d_{298} is the crystal thickness at 298 K, α and β are the first and second order thermal expansion coefficients respectively [11], and T is the temperature of the crystal in Kelvin.

Previous experimental results [12] have shown that for lithium niobate at 632 nm the ordinary and extraordinary refractive indices have a quadratic dependence on temperature. Expressing n_o and n_e in terms of temperature we have [12]

$$n_o = 2.29 - 1.7 \times 10^{-5} T + 3.45 \times 10^{-8} T^2 \quad (5)$$

$$n_e = 2.20 - 2.6 \times 10^{-5} T + 11.2 \times 10^{-8} T^2. \quad (6)$$

Hence we can write

$$\Delta n(T) = n_o - n_e = 0.09 + 9 \times 10^{-6} T - 7.75 \times 10^{-8} T^2. \quad (7)$$

Assuming a simple exponential growth or decay in temperature during the heating or cooling cycle gives

$$T(t) = T_0 + \Delta T \left(1 - e^{-t/\tau} \right) \quad (8)$$

where T is the temperature at time t , T_0 is the initial temperature, ΔT is total temperature change once steady state has been reached, and τ is the characteristic time of the heating / cooling process. Combining Eqs. (3), (4), (7), and (8), we have

$$I_{det}(T) = I_0 e^{-\gamma d} \left\{ \sin \phi \sin \theta + \cos \phi \cos \theta + 2 \sin^2 \phi \sin^2 \theta \cos^2 \phi \cos^2 \theta \cos \left[\frac{2\pi d_0}{\lambda} \left(1 + \alpha (T - 298) + \beta (T - 298)^2 \right) \times \left(\Delta n + \Delta n_1 T + \Delta n_2 T^2 \right) \right] \right\}. \quad (9)$$

Here d and d_0 are the crystal thicknesses at temperature T and initial temperature T_0 , respectively. As is evident from Eq. (9), as the crystal undergoes a temperature change, the intensity function oscillates with an increasing period due to the exponential nature of the temperature. Note, however, over large temperature ranges (> 100 K) higher order polynomial terms need to be included for the temperature dependence of both the refractive index and crystal length.

For modest temperature changes (i.e. $\Delta T \sim 10 - 40$ K) the actual change in temperature change can be obtained using

$$\frac{d_0}{\lambda} \left(1 + \alpha (T - 298) + \beta (T - 298)^2 \right) \times \left(\Delta n + \Delta n_1(T) + \Delta n_2(T)^2 \right). \quad (10)$$

In practice, the temperature change is determined by counting the number of cycles that occur during the heating and cooling cycle. A more precise temperature reading can be obtained by considering portions of oscillation cycles. Determination of fringe fractions is a common task in interferometry, and research has shown that an accuracy as small as 0.01 of a cycle is possible [13]. In our case in lithium niobate, this gives a possible temperature uncertainty of ~ 0.05 K. In the case of a more crude determination of fringe fraction to the $\lambda/4$ level, an uncertainty in temperature of the order of 1.2 K is found.

The theoretical detected intensity given by Eq. (9) on a temperature increase from 273–293 K, is shown in Figure 1. The constant parameter values are shown in Table 1. For simplicity, we have set the attenuation term $e^{-\gamma d} = 1$.

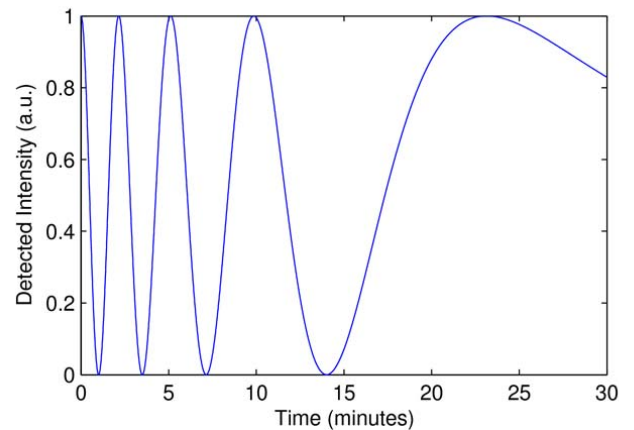


FIG. 1 Oscillations of detected intensity, as predicted by Eq. (9), for a LiNbO₃ crystal of thickness $d_0 = 3$ mm, $\tau = 8$ mins and $\Delta T = 20$ K.

Parameter	Value	Source
α	$1.54 \times 10^{-5} \text{ K}^{-1}$	[11]
β	$5.3 \times 10^{-9} \text{ K}^{-2}$	[11]
Δn	0.09	[14]
Δn_1	$9 \times 10^{-6} \text{ K}^{-1}$	[12]
Δn_2	$-7.75 \times 10^{-8} \text{ K}^{-2}$	[12]

TABLE 1 Typical parameter values for LiNbO₃.

3 EXPERIMENT SETUP AND RESULTS

The experimental setup is shown in Figure 2. The LiNbO_3 :Fe crystal (0.05% mol/wt, $10 \times 8 \times 3 \text{ mm}^3$ ($x \times y \times z$)) was mounted on a heating element, which had a maximum temperature of approximately 50°C . An unexpanded 633 nm beam from an intensity stabilised diode laser propagated through the crystal at an angle of approximately 10° to the normal of the crystal faces and was projected onto a photodetector which had a polariser mounted on its front face for beam attenuation. The angle of incidence of the beam with the crystal was 10° to avoid interference effects on the internal faces. Additionally a 633 nm helium neon beam was collimated and expanded to approximately 6 mm in size and projected through the crystal to a CCD camera attached to a computer. A polariser was also placed in front of the CCD for beam attenuation and as an analyser. The expanded beam was used to observe temperature gradients inside the crystal.

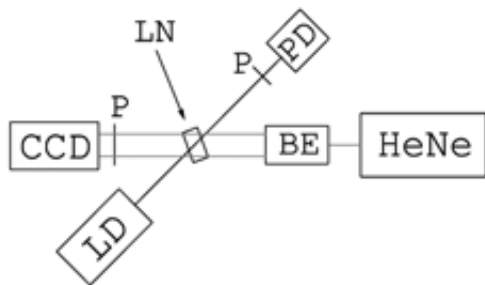


FIG. 2 The experimental layout. LD - laser diode at 633 nm, PD - photodetector, HeNe - Helium Neon laser at 633 nm, BE - beam expander, LN - Lithium niobate crystal, P's - polarisers, CCD - CCD camera attached to computer.

The experimental procedure consisted of monitoring the intensity measured at the photodetector while heating or cooling the lithium niobate crystal. As shown in the theoretical considerations above, the change in temperature affects the birefringence of the crystal, along with its physical size. These effects alter the polarisation state of the beam as it exits the crystal thus an oscillating behaviour is seen in the intensity detected at the photodetector. Figure 4 shows the oscillations in detected intensity, while Figure 3 shows the crystal temperature as measured with a thermocouple, for a temperature change of approximately 20°C . Five complete oscillations can be seen, indicating that each oscillation corresponds to a temperature change of approximately 4°C . Note also that the average detected intensity and oscillation amplitude both reduce over time; this is a consequence of beam fanning, which will be discussed.

The validity of Eq. (9) is demonstrated in Figure 5. Here I_{det} is plotted for the thermocouple-measured temperature values shown in Figure 3. Note that the oscillations take a very similar form to the ones presented in Figure 4. This confirms the theoretical considerations, and verifies that the chosen parameter values are appropriate to our crystal.

Temperature gradients in the crystal were observed using the expanded 633 nm HeNe beam as the probe. Images were captured with the CCD camera at regular time intervals (period ~ 4 seconds) as the temperature of the crystal changed. The

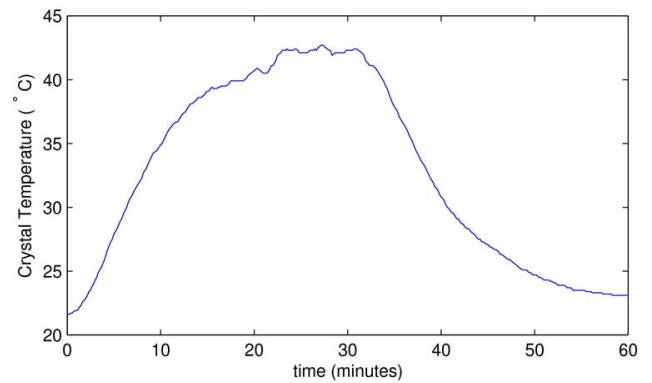


FIG. 3 The measured temperature at the crystal location during a single heating and cooling cycle.

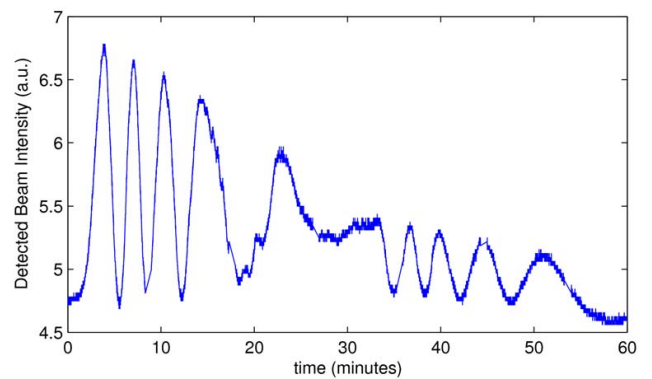


FIG. 4 The detected intensity of the beam after traversing the lithium niobate crystal for the same time scale as Figure 3. The cooling process begins at $t = 30$ min.

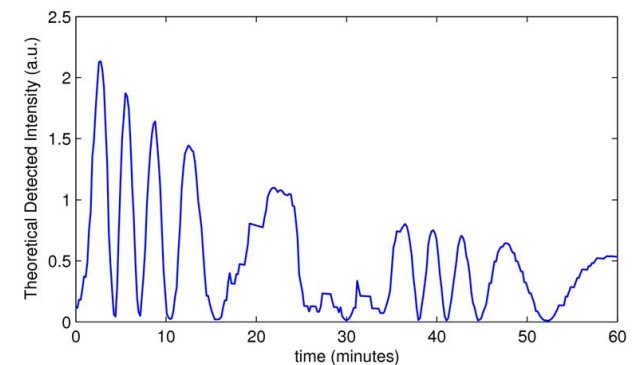


FIG. 5 The theoretical beam intensity as predicted by Eq. (9) using the thermocouple-measured temperature data from Figure 3. The cooling process begins at $t = 30$ min.

same polarisation principle applies to the expanded beam, and since each CCD image covers a $2 \text{ mm} \times 3 \text{ mm}$ region of the crystal, different regions of the image change brightness in a way that is dependent on the temperature change in that region. Qualitatively, since the crystal is heated from underneath we see that lower parts of the CCD images change brightness earlier than higher regions. This effect is noticeable because the thermal conductivity of lithium niobate is quite low [10]. Therefore, by monitoring horizontal regions of the CCD images over time, we see phase and/or period differences in the brightness oscillations of these sections. However, due to slight variations of the refractive index of the crystal in each location, the initial phase of the oscillations at different locations varies. In this case we should take account of the different initial cycle starting points for each strip and calcu-

late the temperature change accordingly. It is necessary only to consider horizontal regions of the CCD images, as significant temperature gradients are expected only in the vertical direction when the heat source is applied to the crystal's lower surface.

Figure 6 shows the oscillations for four such horizontal regions during a heating process. In this case, the $652 \text{ pixel} \times 492 \text{ pixel}$ CCD image was divided into six equal-sized horizontal strips (each 652×82) and the average brightness of each region plotted against time. In this Figure, each of Regions 1–4 corresponds to a quarter of the CCD image from bottom to top of the crystal. Note that Region 4, corresponding to the top of the crystal, displays a noticeable delay in its oscillations. The corresponding temperature change in each region of the crystal is shown in Figure 7. Once again, Region 4 displays a delay in temperature increase when compared with the other regions, as expected since it corresponds to the top of the crystal.

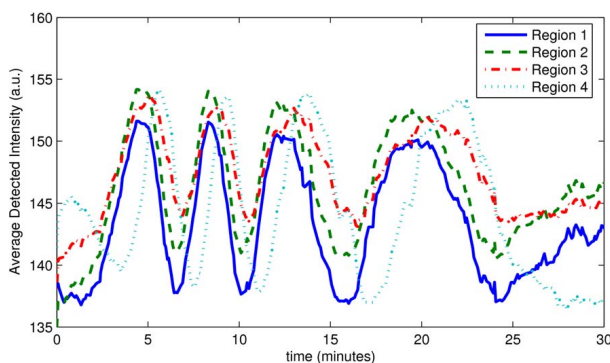


FIG. 6 The measured intensity of different regions of the CCD image (corresponding to different regions of the crystal) during a heating and cooling cycle.

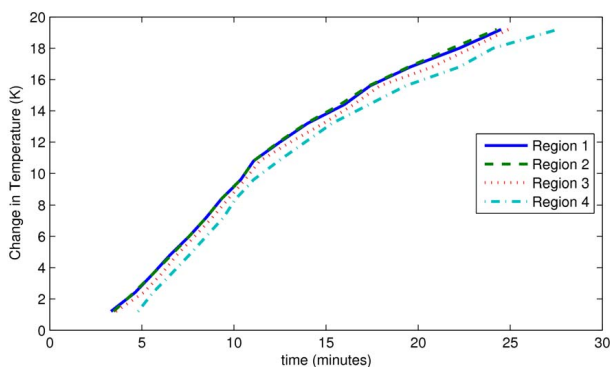


FIG. 7 The measured temperature change of different regions of the crystal during a heating and cooling cycle.

4 DISCUSSION

The experimental results in Figure 4 show that during the cooling process, the oscillation amplitude and average level have dropped when compared with the heating cycle. This is due to beam fanning in the lithium niobate crystal. Beam fanning (or light induced scattering) is a phenomenon that originates from the amplification of scattered radiation as the light field traverses the photorefractive medium [15, 16]. Consequently, this process reduces the amount of light travelling in the original beam direction and as such can be treated like

other loss processes such as absorption. Beam fanning is a useful effect in such applications as self-pumped phase conjugation and in the operation of photorefractive oscillators, but is a hindrance in some applications such as holographic storage [17]. The effect becomes worse with increasing exposure time, since scattered light is itself amplified, causing more scattering, and so on. Beam fanning is a photorefractive effect that is temperature dependent because as the material temperature is increased, hydrogen ions (protons) become mobile and tend to negate the effects of the photorefractive index change [16]. Thus in our treatment of the beam fanning term, beam fanning has both a time and temperature dependence. The effects of beam fanning are incorporated into our derivation for the expected oscillations (Eq. (9)) using the generalised loss coefficient γ . We allow γ to be a time and temperature dependent function

$$\gamma(t) = \gamma_0 \left(1 - e^{-\frac{t}{\tau_f}}\right) e^{-kT(t)} \quad (11)$$

where τ_f is a time constant dependent on the magnitude of the beam fanning effect. During the heating phase, the beam fanning effect tends to be increased due to a longer exposure time, but beam fanning is also reduced due to the temperature increase. These competing effects tend to cancel each other out and the effect of beam fanning is minimal. During the cooling phase; however, both the temperature and exposure time effects act in concert, and the beam fanning effect is extremely pronounced. This is seen clearly in the experimental data in Figure 3, with the decreasing of the average intensity and the amplitude of the oscillations.

The precision of this method of determining temperature change is dependent on a number of factors. The first and foremost is the set of physical parameters of the birefringent crystal used, that is, the expansion and thermo-optic coefficients. With appropriate selection of a birefringent crystal with more suitable values of these parameters, the temperature change corresponding to one full cycle could be decreased, thus increasing the precision of the technique. That being said, one of the most appropriate applications of this technique is when a birefringent crystal is already in use for some other application (e.g. holograms) and one requires to measure the temperature change in the crystal. As a stand-alone method for temperature measure, this technique would be relatively expensive compared to other methods.

The novel application of measuring temperature gradients in the medium is a particular advantage of this method. Along with a useful monitoring technique for stresses in the crystal, one could also take measurements of the thermal conductivity, and heat diffusion coefficients for the material.

5 CONCLUSION

In this paper we have presented a method for remotely determining the temperature change in the photorefractive crystal. The method is based on the birefringence of the crystal and more importantly, the birefringence change of the crystal during a change in temperature. The theory indicates that with known parameter values for lithium niobate, the temperature change in the material can be deduced from the num-

ber of cycles observed in the detected intensity. The uncertainty in this measure could be as low as 0.05 K, but is more likely to be 1.2 K. This value is not as low as typical uncertainties for thermocouple-based temperature probes; however the method offers significant advantages as there is no requirement for obstruction of other beams that may be being used in the crystal (e.g. beams for hologram formation). Furthermore, this method of temperature sensing has a wide range – of the order of 200 K or more, with no sacrifice in precision. An additional advantage is that by using an expanded probe beam, temperature gradients can be observed in the crystal. These could provide useful information on the strains inside the crystal as its temperature is changed as well as determining heat diffusion parameters for the medium.

References

- [1] J. Ashley, M.-P. Bernal, G. Burr, H. Coufal, H. Guenther, J. Hoffnagle, C. Jefferson, B. Marcus, R. Macfarlane, R. Shelby, and G. Sincerbox, "Holographic Data Storage" IBM J. Res. Dev. **44**, 341–368 (2000).
- [2] Y. Kawata, H. Ueki, Y. Hashimoto, and S. Kawata, "Three-dimensional optical memory with a photorefractive crystal" Appl. Optics **34**, 4105 (1995).
- [3] D. Staebler, W. Burke, W. Phillips, and J. Amodei, "Multiple Storage and Erasure of fixed holograms in Fe doped LiNbO₃" Appl. Phys. Lett. **26**, 182–184 (1975).
- [4] C. Hsieh, S. Lin, K. Hsu, T. Hsieh, A. Chiou, and J. Hong, "Optimal conditions for thermal fixing of volume holograms in Fe:LiNbO₃ crystals" Appl. Optics **38**, 6141–6151 (1999).
- [5] K. Buse, S. Breer, K. Peithmann, S. Kapphan, M. Gao, and E. Kratzig, "Origin of thermal fixing in photorefractive lithium niobate crystals" Phys. Rev. B **56**, 1225–1235 (1997).
- [6] D. Staebler and J. Amodei, "Thermally fixed holograms in LiNbO₃" Ferroelectrics **3**, 107–113 (1972).
- [7] A. Medez and L. Arizmendi, "Maximum diffraction efficiency of fixed holograms in lithium niobate" Opt. Mater. **10**, 55 (1998).
- [8] V. Gaba, D. Sugak, and I. Kravchuk, "On the possible application of LiNbO₃ single crystals as temperature indicators on the base of their temperature dependencies of birefringence", in *Optics and Nonlinear Optics of Liquid Crystalline Compounds* pp. 321–324 (SPIE, 1996).
- [9] G. Chartier, *Introduction to optics* (Springer, 2005).
- [10] K. Wong (ed.), *Properties of lithium niobate* (Institute of Engineering and Technology, 2002).
- [11] Y. Kim and R. Smith, "Thermal Expansion of Lithium Tantalate and Lithium Niobate Single Crystals" J. Appl. Phys. **40**, 4637–4641 (1969).
- [12] L. Moretti, M. Iodice, F. Della Corte, and I. Rendina, "Temperature dependencies of the thermo-optic coefficient of lithium niobate, from 300 to 515 K in the visible and infrared regions" J. Appl. Phys. **98**, 036101–05 (2005).
- [13] F. Chau, H. Shang, C. Soh, and Y. Hung, "Determination of fractional fringe orders in holographic interferometry using polarization phase shifting" Opt. Laser Technol. **25**, 371–375 (1993).
- [14] U. Schlarb and K. Betzler, "Refractive Indices of Lithium Niobate as a Function of Temperature, Wavelength, and Composition: A Generalized Fit" Phys. Rev. B **48**, 15613–15620 (1993).
- [15] A. Ashkin, G. Boyd, J. Dziedzic, R. Smith, A. Ballman, J. Levinstein, and K. Nassau, "Optically-induced refractive index inhomogeneities in LiNbO₃ and LiTaO₃" Appl. Phys. Lett. **9**, 72–74 (1966).
- [16] F. Zhao, H. Zhou, Z. Wu, F. Yu, and D. McMillen, "Temperature dependence of light-induced scattering in a Ce:Fe:LiNbO₃ photorefractive crystal" Opt. Eng. **35**, 1985–1992 (1996).
- [17] F. Mok, "Angle-multiplexed storage of 5000 holograms in lithium niobate" Opt. Lett. **18**, 915–917 (1993).